

# Optimization of Rheology Parameters for Feedstock by Powder Injection Molding (PIM) Via Taguchi Analysis

Levent Urtekin<sup>1</sup>, Faik Yılan<sup>1\*</sup>, İbrahim Baki Şahin<sup>1</sup>

<sup>1</sup>Department of Mechanical Engineering,  
Kirsehir Ahi Evran University, Kirsehir, 40100, TURKEY

\*Corresponding Author

DOI: <https://doi.org/10.30880/ijie.2023.15.07.009>

Received 14 June 2023; Accepted 16 October 2023; Available online 5 December 2023

**Abstract:** The most critical process in the powder injection molding method is determining the powder/binder rate and its properties. The most important feature that distinguishes the powder injection molding method from other powder metallurgy production methods is its advantage in producing high raw density and complex shaped parts. However, providing these advantages includes a multi-parameter process that directly affects the injection molding parameters and the final part's mechanical properties. In addition, the difficulty of experimental studies causes energy, time, and cost losses in determining the powder/binder rate and rheological properties of the feedstock so that the advantages of the method turn into a manageable disadvantage. This study performed rheology studies for three different feedstocks (PW/CW/SA, PW/PE/SA, and PEG8000/PP/SA). In this context, this paper determined the rheological properties of different feedstocks to take advantage of the Taguchi analysis. Flow behavior index, viscosity and optimum loading rates were determined separately for all feedstocks. The results exhibited the injection molding can be done with the determined best (58% steatite+PEG8000/PP/SA) F3 feedstock by weight. Based on it was found that viscosity and melt flow index were not a problem for injection molding in three different feedstocks used in the result, advantages and disadvantages were observed.

**Keywords:** Powder injection molding (PIM), rheology, feedstocks, Taguchi method, optimization

## 1. Introduction

Powder injection molding (PIM) is a mass production process of machine parts with complex geometries using both metal and ceramic powders [1]. PIM technique is used to fabricate a wide diversity of parts for high temperature application areas, especially in the aerospace industry, healthcare devices, and automotive industry [2], [3], [4]. This manufacturing method involves three stages. Initially, appropriate thermoplastic binder and powder amounts are determined and mixed. Afterwards, there are injection molding, debinding and sintering. The each stage must be controlled [5], [6], [7].

PIM process, successful flow and trouble-free molding depends primarily on the viscosity and rheological behavior of the feedstock [8], [9], [10], [11]. Viscosity is calculated with the help of the Eq. given in Eq. 1. Here  $\eta$  denotes viscosity,  $\tau$  shear stress (Pa), and  $\dot{\gamma}$  shear rate ( $s^{-1}$ ).

$$\eta = \frac{\tau}{\dot{\gamma}} \quad (1)$$

This method, it is desirable for the flow type to exhibit pseudoplastic fluid. In pseudoplastic flow behavior, viscosity decreases as shear rate increases, and it performs better in filling mould [12], [13]. Wei et al. [14] used feedstocks consisting of a polypropylene (PP)/paraffin wax (PW)/stearic acid (SA) mixture and achieved pseudoplastic behavior at the optimum temperature of 170°C of the materials. Urtekin et al. [15] stated that the optimum powder loading is 55%

by volume, with two different polypropylene/polyethylene (PP/PE) binders as the skeleton binder, without changing the main binder polyethylene glycol (PEG4000). The viscosity value is below 1000 Pa.s in both feedstocks exhibiting optimum loading.

The majority of defects that can deteriorate the quality of green parts are due to their rheological properties, and are therefore deformations can occur such as voids, cracks, swelling, and warping. For example, Supati et al. [16] reported that inhomogeneous feedstock's cause distortion in the molded part. Similarly, Thomas-Vielma et al. [17] stated that during the removal of paraffin from the binder system consisting of polyethylene (HDPE)/PW/SA at relatively low temperature, the main binder HDPE maintains its solid state, providing the necessary strength and minimizing errors. Subaşı et al. [18] carried out a study on the rheological behavior and molding parameters of a Ti-6Al-4V based feedstock. The main findings from this study revealed that the moldability index was higher than 57-59% powder loading by volume. However, Thavanayagam and Swan [19] developed a new rheological model that includes the flow properties of raw materials obtained from rheological tests that have low production costs. Consequently, PIM process is affected by various factors, so it requires a series of experiments to obtain suitable parameters. Consequently, PIM process is affected by various factors, so it requires a series of experiments to obtain suitable parameters.

Taguchi method is a statistical approach and it is to obtain data by keeping one parameter constant in a certain process and changing other parameters each time. With the Taguchi method, the number of experimental studies to be carried out in a laboratory environment is minimized. Thus, experimental cost is reduced. Ji et al. [20] was reported the effect of three sintering factors on the final density using the Taguchi method. Wahi et al. [21] optimized the palm stearin and polyethylene linker system with several injection parameters in the L18 orthogonal array by Taguchi. Chua et al. [22] obtained the best quality green parts by optimizing the injection and binder parameters. Park et al. [23] performed a minimal number of experimental studies by analyzing the powder-binder separaten behavior with the Taguchi method. In this regard, the main aim of this study is Taguchi method. However, the effect of the method on powder metallurgy is detailed in ref. [24]. The knowledge gained by optimizing the amount of powder and binders helps engineers, industrialists and scientists save time, materials and energy.

Rheology study is the most critical stage of the PIM method. It is necessary to determine the flow properties of the feedstocks obtained with the powder/binder mix. Optimum powder/binder mixtures are obtained by increasing the amount of powder and decreasing the binders. However, this mixture should not adversely affect the mold filling, binder removal, and sintering processes. The viscosity is expected to be in the range of 100-1000 Pa.s. The powder/binder rate is preferably 50-50%. The use of critical powder loading below 2-5% as optimum powder loading makes a significant contribution to the molding and final production processes. The rheological study is of great importance due to the reasons stated. Determining the powder/binder mixture rate in this rheological study requires serious effort and experience. In this study, it is expected that preliminary analyzes of rheological experiments will be made by performing Taguchi analysis and realistic results will be achieved in a shorter time (cost and energy saving). By transferring the data obtained from this study to moldflow simulation analysis in future studies, it is expected to obtain healthy results in practice by selecting mold design, mold filling, shrinkage and temperature parameters. In the study, both the optimum mixing value for three different binders and the determination of the ideal solid loading rate within the binders were provided. The purpose of this paper is to optimize the different rheological parameters to be used in the PIM process with the Taguchi method. In particular, effect of different binders, temperatures and solid loading rates on the rheological properties of a PIM feedstock is presented. Thus, optimum melt flow indices and viscosity values have been determined. This information will continue to expand a new market in competing industrial applications for manufacturing PIM parts.

## 2. Experimental Methods

### 2.1 Experimental Setup

Powder size and form is an important parameter for Powder Injection Molding (metal and ceramics). Especially for metals, spherical powders with an average powder size below 20 microns provide high packaging density. It is known that powder size distribution affects the packing density, and it is important literature information that the packing density obtained before sintering affects the density in the final piece. A spherical powder shape is required for powder metal parts with high density. 80% of the powders used in powder metallurgy are in spherical shape. As a result of the analyzes carried out at Dumlupınar University Advanced Technologies and Design Center, the suitability of the Ti-6Al-4V material for Metal Injection Molding was determined by performing average powder size and powder size distribution, powder form (SEM images), and EDS analyses (Fig. 1). As a result of the analysis, it was seen that the average powder size was around 13.4 microns and was spherical. In EDS analyses, it was determined that the powder provided was Ti-6Al-4V alloy. The used binder component systems and binder elements in this study are illustrated in Table 1 and Table2, respectively. Stearic acid was preferred as the lubricant in these feedstocks. This is because it aids the wettability of the flow between the binder [25].

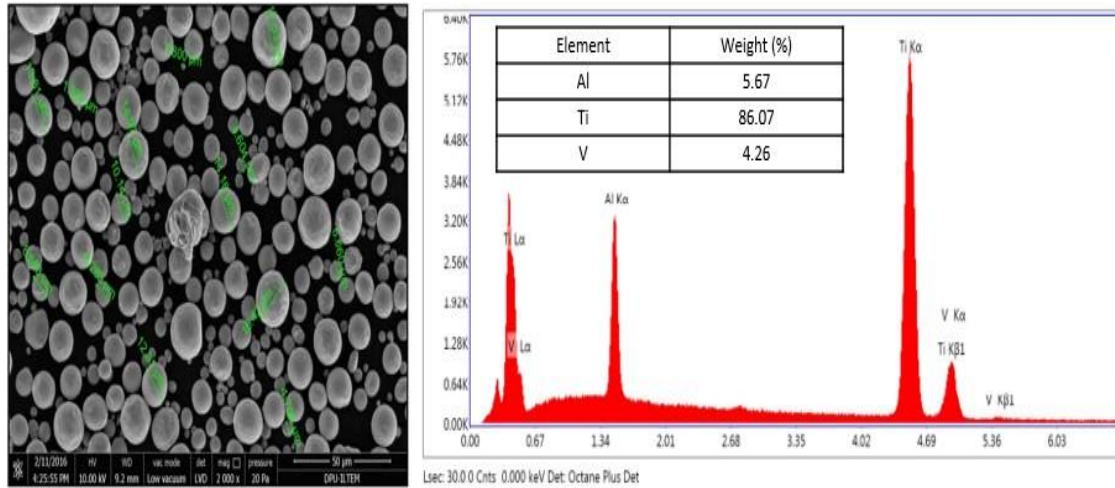


Fig. 1 – SEM and EDS analysis

Table 1 - Binder systems used in the experimental study

Feedstocks	Solid loading rate (Weight %)	Main binder	Skeleton binder	Lubricant
		65%	30%	5%
F1	49-54	Paraffin wax, PW	Carnauba wax, CW	Stearic acid, SA
F2	47-57	Paraffin wax, PW	Polyethylene, PE	Stearic acid, SA
F3	50-60	Polyethylene glycol, PEG8000	Polypropylene, PP	Stearic acid, SA

Table 2 - Binder elements

Binders Elements	Vendor	Density (g/cm <sup>3</sup> )	Melting Point (°C)	Weight (%)
Polyethylene glycol, PEG8000	Alfa Aser	1,204	60-63	65
Polypropylene, PP	Petkim A.Ş.	0,85	189	30
Polyethylene, PE	Petkim A.Ş.	0,91	137	30
Paraffin wax, PW	Merck	0,9	42-72	60
Stearic acid, SA	Merck	0,94	68-70	5

Rheology experiments were carried out in accordance with ASTM D1238 standards using a Protherm brand rheometer device (capillary rheometer). The features of this device are; cylinder length is 115 mm, inner diameter is 10 mm, piston length is 6.35 mm, die length is 8 mm and diameter is 2 mm. Before starting the experiments, the device was first cleaned. Then, the cylinder and piston temperature was kept constant at  $80-260 \pm 0,5$  °C for 15 minutes, ensuring that there was no change in the temperature value during the experiment. After a certain period of time, the first parts flowing from the binders placed in the cylinder and the air bubbles formed in it are removed. Appropriate feedstocks (at least three) are then weighed to mg precision, respectively, and an average weight determined. If the difference between the largest and smallest values is more than 10% of the average weight, the test results are neglected and the experiments are repeated with new binder systems. Volumetric solid loading rates varying between 47-60% were prepared for three different binder mixtures and the prepared mixtures were granulated by passing through the extruder. Granulated mixtures were passed through a capillary rheometer and the rheological character of each feedstock was determined. Melt flow indices and viscosity values were calculated for three different feedstocks.

## 2.2 Taguchi Experimental Design

The most suitable parameter set for the investigated conditions was evaluated with the Taguchi method. The experimental parameters and levels of the feedstocks are given in Table (3), (5), and (7) respectively. For F1 feedstock, each factor is set to 4 levels, while for F2 and F3 feedstocks, each factor is designed to be 5-level. The aim of the experimental study was to determine the ideal feedstock for binder systems formed in different parameters. In this method, orthogonal array is used to understand the effect of each factor with the minimum number of experiments (Table

(4), (6), and (8)). The variation value obtained from the experimental study is converted to the signal-to-noise (S/N) rate. S/N rate is calculated according to the formulas given in Eqs. (2), (3), and (4).

Smaller is better;

$$\frac{S}{N} = -10 \log\left[\left(\frac{1}{n}\right) \sum (y^2)\right] \tag{2}$$

Nominal is better;

$$\frac{S}{N} = 10 \log\left(\frac{\bar{y}}{s_y^2}\right) \tag{3}$$

Larger is better;

$$\frac{S}{N} = -10 \log\left[\left(\frac{1}{n}\right) \sum \left(\frac{1}{y^2}\right)\right] \tag{4}$$

In these Eqs, n represents the number of experiments, y the observed data,  $\bar{y}$  the mean of the observed data [26]. In addition, the unit of S/N rate is percent.

**Table 3 - The parameters and the values corresponding to their levels studied in F1**

Factors	Levels			
	1	2	3	4
Temperature (°C)	80	90	100	-
Solid loading rate (%)	49	51	53	54

**Table 4 - Chosen L<sub>12</sub> experimental plan**

Feedstocks (Binder component system)	Experiment no.	Experiment value	
		Temperature (°C)	Solid loading rate (%)
F1 PW/CW/SA	1	80	49
	2	80	51
	3	80	53
	4	80	54
	5	90	49
	6	90	51
	7	90	53
	8	90	54
	9	100	49
	10	100	51
	11	100	53
	12	100	54

**Table 5 - The parameters and the values corresponding to their levels studied in F2**

Factors	Levels				
	1	2	3	4	5
Temperature (°C)	180	190	200	210	220
Solid loading rate (%)	47	50	55	57	-

### 3. Results and Discussion

#### 3.1 ANOVA Analysis for F1 Feedstock

Analysis of variance (ANOVA) forcing methods is used in interpreting experimental data and determining the effects of the rates of the parameters. ANOVA test is a statistical tool used to reveal the difference between the average performances of the created parts groups. ANOVA shows which parts are adequate on which process and in what performance. The analysis of variance aims to reveal how much the examined elements progress, the output values chosen to measure quality, and what kinds of various levels cause [20]. The melt flow index ANOVA for F1 are given in Table 9.

**Table 6 - Chosen L<sub>20</sub> experimental plan**

Feedstocks (Binder component system)	Experiment no.	Experiment value	
		Temperature (°C)	Solid loading rate (%)
F2 PW/PE/SA	1	180	47
	2	180	50
	3	180	55
	4	180	57
	5	190	47
	6	190	50
	7	190	55
	8	190	57
	9	200	47
	10	200	50
	11	200	55
	12	200	57
	13	210	47
	14	210	50
	15	210	55
	16	210	57
	17	220	47
	18	220	50
	19	220	55
	20	220	57

**Table 7 - The parameters and the values corresponding to their levels studied in F3**

Factors	Levels				
	1	2	3	4	5
Temperature (°C)	180	190	200	210	220
Solid loading rate (%)	50	55	58	60	-

Table 9 shows that the temperature for the F1 mixture has a statistical effect of 59.17% on the melt flow index, and the solid loading rate has an effect of 37.89%. Therefore, it is understood that the temperature is much more effective when we look at the P value (P<0). The relationship between control and experimental factors in regression analysis experimental studies is seen in Eq. (5).

$$MFI \left( \frac{g}{10min} \right) = 1865 + 17,70 Temp. °C - 60,16 Mixing rate(\%) \tag{5}$$

The relationship between the values calculated with the help of this Eq. 5 and the actual measurement results has been examined. Viscosity analysis results for F1 feedstock are indicated in Table 10. The F rate establishes at a certain confidence level whether the process parameter is critical. A higher value of the F-rate indicates that any small change

in the process parameter can significantly impact the performance characteristics. It is understood that the solid loading rate has the most significant effect on the viscosity. Table 10 shows that for the F1 mixture, the temperature has a statistical effect of 24.59% and the solid loading rate of 70.17% on the viscosity. Regression analysis shows the relationship between control and experimental factors in experimental studies in Eq. (6).

$$Viscosity(Pa.s) = -8413 - 31,2 Temp. ^\circ C + 230,5 Mixing\ rate(\%) \tag{6}$$

**Table 8 - Chosen L<sub>20</sub> experimental plan**

Feedstocks (Binder component system)	Experiment no.	Experiment value	
		Temperature (°C)	Solid loading rate (%)
F3 PEG8000/PP/SA	1	180	50
	2	180	55
	3	180	58
	4	180	60
	5	190	50
	6	190	55
	7	190	58
	8	190	60
	9	200	50
	10	200	55
	11	200	58
	12	200	60
	13	210	50
	14	210	55
	15	210	58
	16	210	60
	17	220	50
	18	220	55
	19	220	58
	20	220	60

**Table 9 - ANOVA Analysis Results for Melt flow index (g/10min.), F1**

Source	DF	Adj SS	Adj MS	F-Value	P-Value	% Contribution
Temperature (°C)	2	251273	125636	60,7	0	59,17639
Solid loading rate (%)	3	160925	53642	25,92	0,001	37,89886
Error	6	12419	2070	-	-	2,924753
Total	11	424617		-	-	100

R-Sq. =96,75% R-Sq. (adj) =96,02% R-sq(pred)=94.90%

**Table 10 - ANOVA Analysis Results for Viscosity (Pa.s), F1**

Source	DF	Adj SS	Adj MS	F-Value	P-Value	% Contribution
Temperature (°C)	2	865774	432887	14,08	0,005	24,59008
Solid loading rate (%)	3	2470574	823525	26,78	0,001	70,17028
Error	6	184480	30747	-	-	5,239678
Total	11	3520827		-	-	100

R-Sq. =88,98 % R-Sq. (adj) =86,53 % R-sq(pred)=78,60%

There are some techniques in the evaluation of the experimental results with Taguchi. The planning of the experiments with the determined parameters, the determination of the effect levels of the experimental parameters on the obtained test results, and the determination of the optimum test parameters can be done with the Taguchi method. Taguchi converts the objective function values to the signal-to-noise (S/N) rate to measure the performance characteristic of the levels of control factors versus factors. The S/N rate is defined as the desired signal rate for the unwanted random noise value and shows the quality characteristics of the experimental data [19]. With this analysis, it was preferred to evaluate the viscosity as "small is better" and for melt flow index and "largest is better," Fig. 2a, shows the main effect plot for the S/N rate for the melt flow index. When Fig. 2a, is examined, it can be estimated that the best melt flow index can be obtained in parameter conditions where the temperature is 100 (°C), and the solid loading rate is 49%. Figure 2 shows the main effect plot for the S/N rate for viscosity. When Fig. 2b is examined, it can be estimated that the best viscosity can be obtained in parameter conditions where the temperature is 80 (°C), and the solid loading rate is 54%.

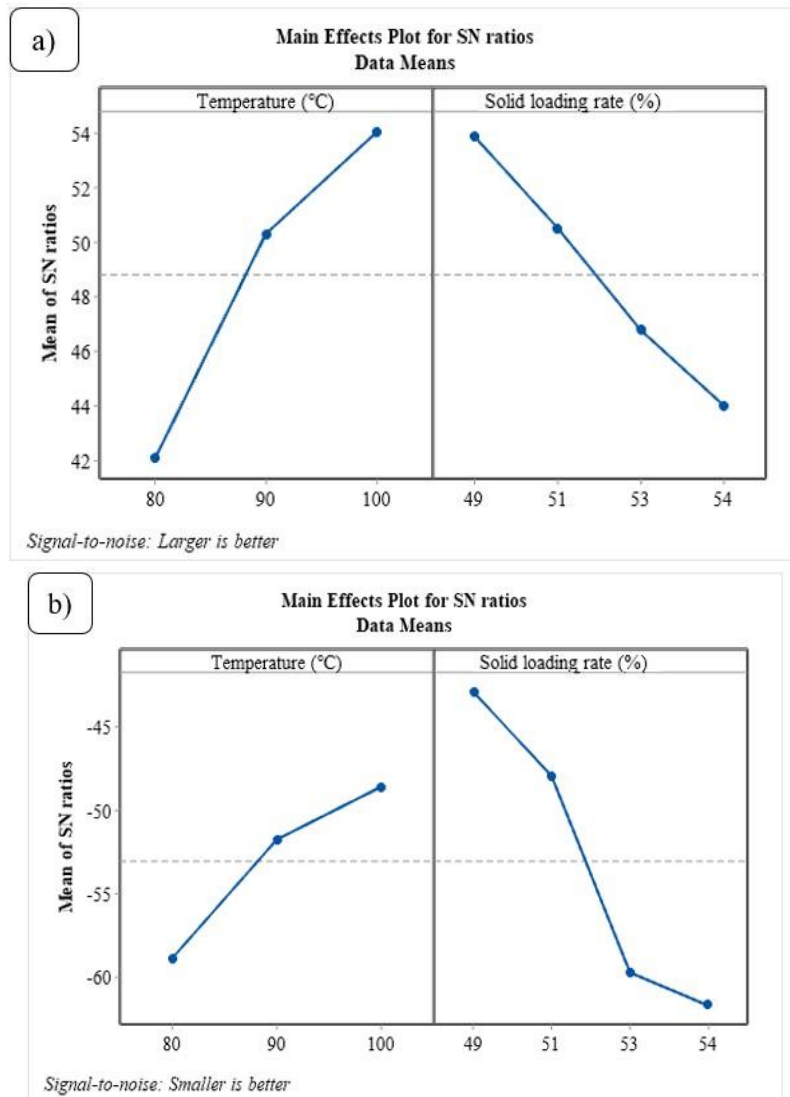


**Fig. 2 - Taguchi analysis (a) melt flow index (g/10min.); (b) viscosity (Pa.s), F1**

Contour charts, using different colors for different response ranges, estimate the effect of two factors on a single response simultaneously. Fig. 3a and 3b, show the effect of temperature and solid loading rate on the melt flow index. The response range by color coding is also shown in Fig. 3a. When the temperature is 95-100 °C, the Melt flow index-solid loading rate is > 600 (g/10min.) at 49%, 500-600 (g/10min.) at 51%, and 400-500 (g/10min.) at 53%, in 54%, it is between 300-400 (g/10min.). It shows the maximum melt flow index at a low solid loading rate value and high-temperature value. Fig. 3b, shows the effect of temperature and solid loading rate on viscosity. When the temperature is 80-85 °C, the viscosity is > 300 (Pa.s) when the solid loading rate is 49%, 300-600 (Pa.s) at 51%, 1200-1500 (Pa.s) at 53%, 54 in %, it is between 1500-1800 (Pa.s). The response range by color coding is also shown in Figure 3.

### 3.2 ANOVA Analysis for F2 Feedstock

ANOVA results for the melt flow index are given in Table 11. Table 11 shows that for the F2 mixture, the temperature has a statistical effect of 75.60% on the melt flow index, and the solid loading rate has an effect of 20.92%. Therefore, it is understood that the temperature is much more effective when we look at the F value in the table.

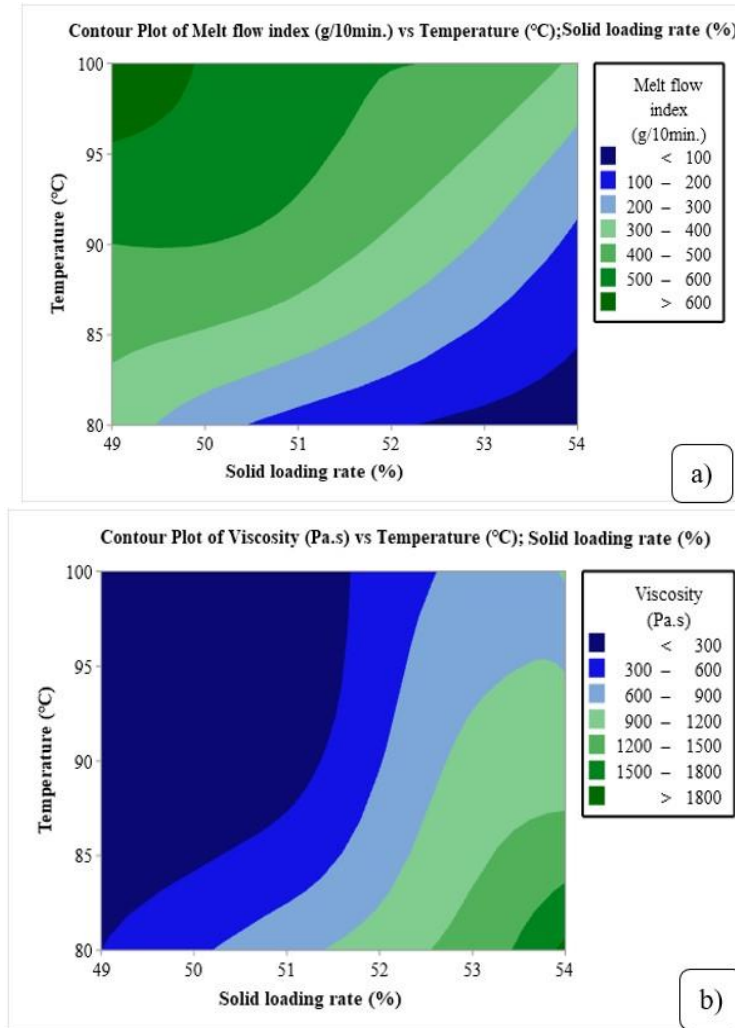


Fig. 3 - Contour plot for (a) melt flow index; (b) viscosity, F1

Table 11 - ANOVA analysis results for melt flow index (g/10min.), F2

Source	DF	Adj SS	Adj MS	F-Value	P-Value	% Contribution
Temperature (°C)	4	1156611	289153	65,32	0	75,60266
Solid loading rate (%)	3	320123	106708	24,1	0	20,92505
Error	12	53122	4427	-	-	3,472355
Total	19	1529855	-	-	-	100

R-Sq. =96,28 % R-Sq. (adj) =95,84 % R-sq(pred)=95,52%

Regression analysis shows the relationship between control and experimental factors in experimental studies in Eq. (7). The relationship between the values calculated with the help of this Eq. 7 and the actual measurement results has been examined.

$$MFI \left( \frac{g}{10min.} \right) = -1183 + 17 Temp.^{\circ}C - 31,82 Mixing\ rate(\%) \tag{7}$$

In Table 12, the viscosity analysis results for F2 are given. Table 12 shows that for the F2 mixture, the temperature has an effect of 67.99%, and the solid loading rate has an effect of 25.08% on viscosity.



**Table 12 - ANOVA analysis results for viscosity (Pa.s), F2**

Source	DF	Adj SS	Adj MS	F-Value	P-Value	% Contribution
Temperature (°C)	4	1017225	254306	29,47	0	67,99278
Solid loading rate (%)	3	375314	125105	14,5	0	25,08653
Error	12	103539	8628	-	-	6,920695
Total	19	1496078		-	-	100

R-Sq. =88,08 % R-Sq. (adj) =86,68 % R-sq(pred)=82,17%

The higher value of the F-rate in the table indicates that any small change in the process parameter can significantly influence the performance characteristics. It is understood that temperature has the most significant effect on viscosity. Regression analysis shows the relationship between control and experimental factors in experimental studies in Eq (8).

$$Viscosity(Pa. s) = 1866 - 15,7 Temp. °C + 32,21 Mixing rate(\%) \tag{8}$$

Fig. 4a, shows the main effect plot for the S/N rate for the melt flow index. When Fig. 4a, is examined, it can be estimated that the best melt flow index can be obtained in parameter conditions where the temperature is 220 (°C), and the solid loading rate is 47%. Fig. 4b, shows the main effect plot for the S/N rate for viscosity. When Fig. 4b, is examined, the best viscosity can be obtained under parameter conditions where the temperature is 220 (°C), and the solid loading rate is 47%.

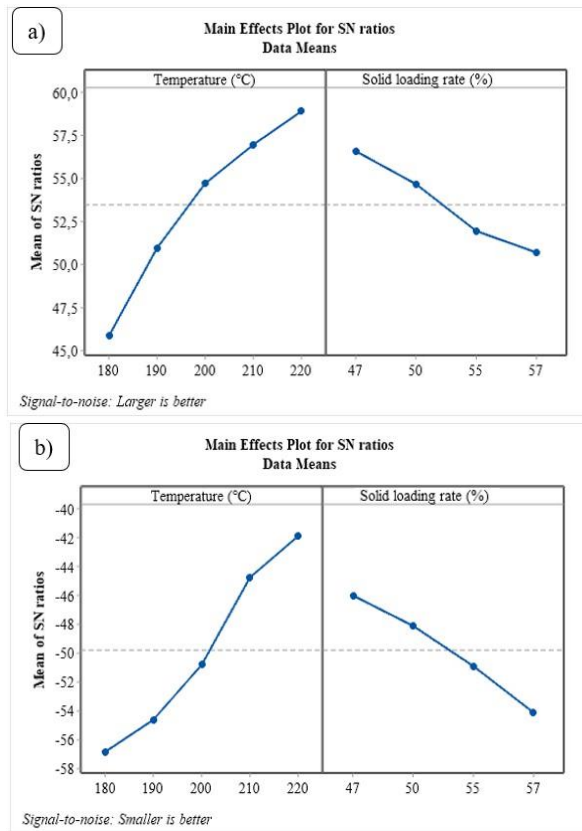


**Fig. 4 - Taguchi analysis (a) melt flow index (g/10min.); (b) viscosity (Pa.s), F2**

Fig. 5a and 5b, show the effect of temperature and solid loading rate on the melt flow index. The response range by color coding is also shown in Fig. 5a. When the temperature is 210-220 °C, melt flow index solid loading rate is > 1000 (g/10min.) at 47%, 800-1000 (g/10min.) at 50%, 800-1000 (g/10min.) at 55%, in 57%, it is between 600-800 (g/10min.). It shows maximum melt flow index at low solid loading rate value and high temperature value. Fig. 5b, shows the effect of temperature and solid loading rate on viscosity. In the case of temperature 180-190 °C, the viscosity is 400-600 (Pa.s) when the solid loading rate is 47%, 400-600 (Pa.s) at 50%, 600-800 (Pa.s) at 55%, 57% at, it is between >1000 (Pa.s). The response range according to color-coding is also shown in Fig 5b.

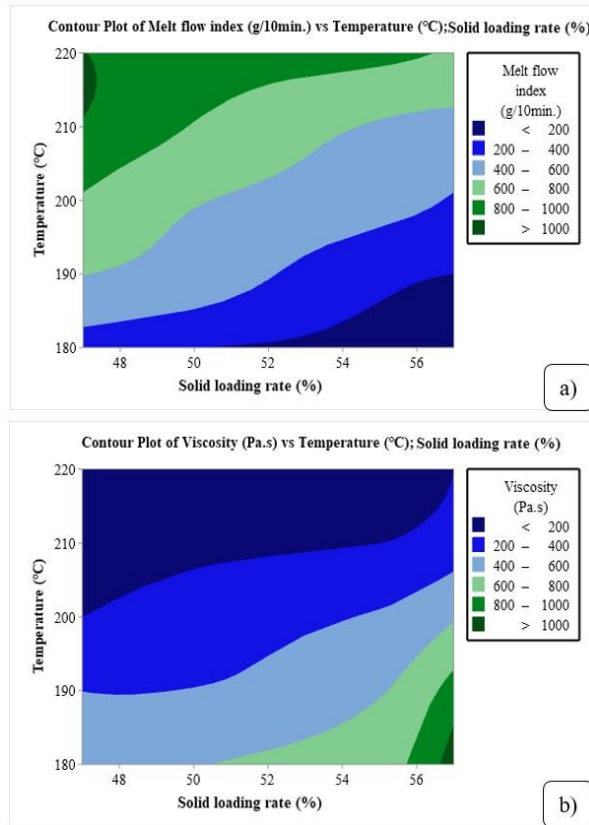


Fig. 5 - Contour plot for (a) melt flow index; (b) viscosity, F2

### 3.3 ANOVA Analysis for F3 Feedstock

ANOVA analysis results for the melt flow index are given in Table 13. When Table 13. was examined, F values can be seen that the solid loading rate is much more effective. For the F3 mixture, it is seen that the temperature has a statistical effect of 29.04%, and the solid loading rate has an effect of 66.67% on the melt flow index.

Table 13 - ANOVA Analysis Results for Melt flow index (g/10min.), F3

Source	DF	Adj SS	Adj MS	F-Value	P-Value	% Contribution
Temperature (°C)	4	798499	199625	20,38	0	29,04541
Solid loading rate (%)	3	1833096	611032	62,38	0	66,67889
Error	12	117544	9795	-	-	4,275664
Total	19	2749140		-	-	100

$$R\text{-Sq.}=91,97\% \quad R\text{-Sq. (adj)}=91,03\% \quad R\text{-sq(pred)}=88,04\%$$

Regression analysis shows the relationship between control and experimental factors in experimental studies in Eq. (9).

$$MFI \left( \frac{g}{10min.} \right) = 2523 + 14,03 \text{ Temp. } ^\circ\text{C} - 78,33 \text{ Mixing rate}(\%) \tag{9}$$

The relationship between the values calculated with the help of this Eq. 9 and the actual measurement results has been examined. Viscosity ANOVA analysis results for F3 feedstock are given in Table 14. Table 14 shows that for the F3 mixture, the temperature has an effect of 38.11% and the solid loading rate of 50.65% on viscosity. A higher value of the F-rate indicates that any small change in the process parameter can significantly affect the performance characteristics. It is understood that the solid loading rate has the most significant effect on the viscosity. Regression analysis shows the relationship between control and experimental factors in experimental studies in Eq. (10).

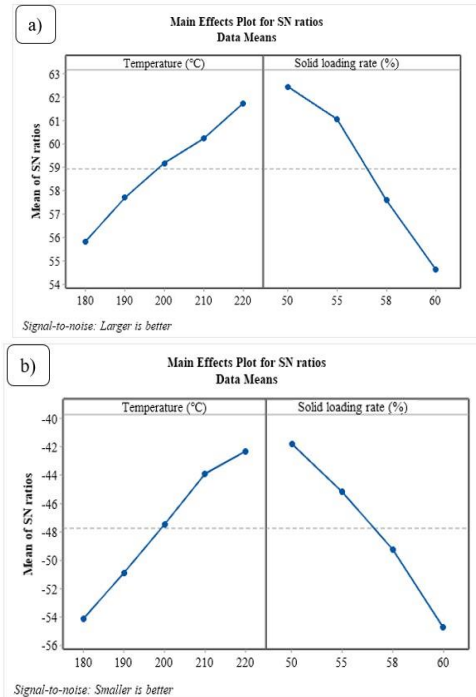
$$Viscosity(Pa.s) = 153 - 11 \text{ Temp. } ^\circ\text{C} + 42,40 \text{ Mixing rate}(\%) \tag{10}$$

**Table 14 - ANOVA analysis results for viscosity (Pa.s), F3**

Source	DF	Adj SS	Adj MS	F-Value	P-Value	% Contribution
Temperature (°C)	4	501311	125328	10,18	0,001	38,11289
Solid loading rate (%)	3	666306	222102	18,04	0	50,65687
Error	12	147715	12310	-	-	11,23024
Total	19	1315332		-	-	100

R-Sq. =75,31 % R-Sq. (adj) =72,40 % R-sq(pred)=64,37%

Fig. 6a, shows the main effect plot for the S/N rate for the melt flow index. When Fig. 6a, is examined, it can be estimated that the best melt flow index can be obtained under the parameter conditions where the temperature is 220 (°C), and the solid loading rate is 50%. Fig. 6b, shows the main effect plot for the S/N rate for viscosity. When Fig. 6b, is examined, the best viscosity can be obtained in parameter conditions where the temperature is 180 (°C), and the solid loading rate is 60%. Fig. 7a and b, show the effect of temperature and solid loading rate on the melt flow index. The response range by color coding is also shown in Fig. 7a. When the temperature is 210-220 °C, the melt flow index solid loading rate is 50% > 1750 (g/10min.), 1250-1500 (g/10min.) at 55%, and 750-1000 (g/10min.) at 58%, at 60%, it is between 750-1000 (g/10min.). It shows the maximum melt flow index at a low solid loading rate value and high-temperature value. Fig. 7b, shows the effect of temperature and solid loading rate on viscosity. When the temperature is 180-190 °C, the viscosity is 200-400 (Pa.s) when the solid loading rate is 50%, 200-400 (Pa.s) at 55%, 400-800 (Pa.s) at 58%, at 60%, it is between 800-1000 (g/10min.). The response range by color-coding is also shown in Fig. 7b.

**Fig. 6 - Taguchi analysis (a) melt flow index (g/10min.); (b) viscosity (Pa.s), F3**

#### 4. Conclusions

In this study, the highest powder content and viscosity values of less than 1000 Pa.s were taken into account in the feedstock analysis. Because of the analysis made, the following conclusions were reached:

1. When the findings obtained as a result of the analyzes are interpreted, the viscosity value range of F1 feedstock at maximum powder loading (54%) is 1500-1800 Pa.s, the viscosity value of F2 feedstock is >1000 (Pa.s) at maximum powder loading (57%), F3 feedstock Viscosity value range at maximum powder loading (60%) was determined as 800-1000 Pa.s.
2. F2 and F3 feedstocks are evaluated in terms of melt flow index at the highest powder loading; the MFI value range of F2 feedstock is 600-800 g/10min., The MFI value range of F3 feedstock is 750-1000 g/10min. has been determined. In terms of MFI value, it has been seen that the F3 feedstock is ideal, preferable in terms of injection molding, binder removal, and sintering.

3. When the viscosity and melt flow index are evaluated together, it is seen that the F3 feedstock is preferable in terms of injection molding, binder removal and sintering.
4. Feedstocks with low viscosity will not be preferred in molding, especially since the low viscosity value in the mold will cause gaps during molding. The use of feedstock mixtures with similar properties in molding will be a disadvantage, as feedstock mixtures with low powder and high binder content will create severe problems during both binder removal and sintering.

Since the R-sq (pred) values found in the regression analysis results are pretty high, using these Eqs. for F1, F2, and F3, feedstocks, predictions can be made for any level of temperature and solid loading rate by using these Eqs. in determining the both melt flow index, and viscosity values without experimenting in future studies.

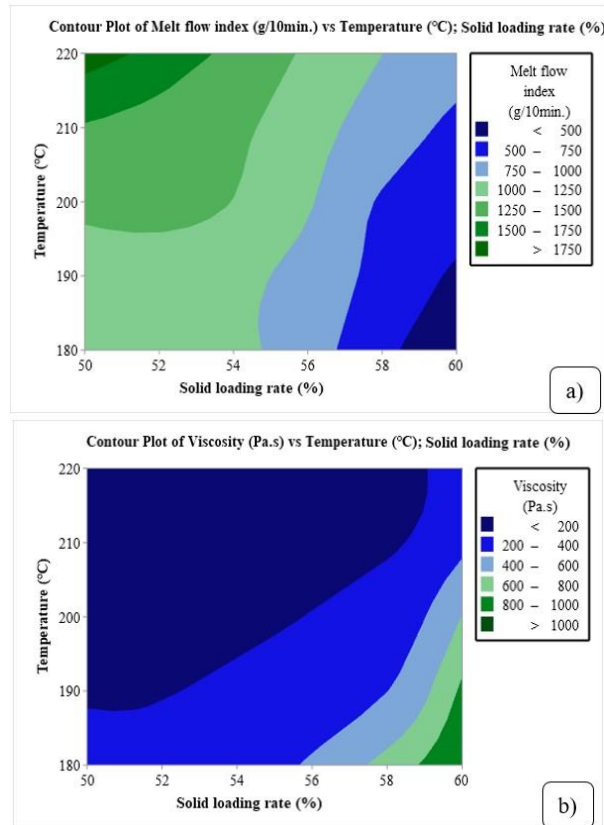


Fig. 7 - Contour plot for (a) melt flow index, and; (b) viscosity, F3

## Acknowledgement

The authors would like to thank Prof. Dr. İbrahim USLAN, for his invaluable support, encouragement and guidance.

## References

- [1] Hausnerová, B. (2009). Powder injection moulding for automotive applications - An alternative to traditional processing routes. *Chem List* 103.
- [2] Technology, J., & Diefendorf, R. J. (1990). Aerospace Industry is Major Focus of Composites Research in Japan. *MRS Bull* 15:50–51. <https://doi.org/10.1557/s0883769400059741>.
- [3] Thavanayagam, G., Pickering K. L, Swan J. E, & Cao P. (2015). Analysis of rheological behaviour of titanium feedstocks formulated with a water-soluble binder system for powder injection moulding. *Powder Technol* 269:227–232. <https://doi.org/10.1016/j.powtec.2014.09.020>.
- [4] Urtekin, L., Genç, A., & Bozkurt, F. (2019). Fabrication and simulation of feedstock for titanium-powder injection-molding cortical-bone screws. *Mater Tehnol* 53:619–625. <https://doi.org/10.17222/mit.2018.088>
- [5] Urtekin, L., Usilan, I., & Tuç, B., (2012). Investigation of effect of feedstock rheologies for injection molding of steatite. *J Fac Eng Archit Gazi Univ* 27:333–341.
- [6] Langlais, D., Demers, V., & Brailovski, V. (2022). Rheology of dry powders and metal injection molding feedstocks formulated on their base. *Powder Technol* 396:13–26. <https://doi.org/10.1016/j.powtec.2021.10.039>.
- [7] Moghadam, MS., Fayyaz, A., & Ardestani, M., (2021). Fabrication of titanium components by low-pressure powder injection moulding using hydride-dehydride titanium powder. *Powder Technol* 377:70–79. <https://doi.org/10.1016/j.powtec.2020.08.075>.

- [8] Li, Y., Huang, B., & Qu, X., (1999). Viscosity and melt rheology of metal injection moulding feedstocks. *Powder Metall* 42:86–90. <https://doi.org/10.1179/pom.1999.42.1.86>.
- [9] Suri, P., Atre, S. V., German, R. M., & de Souza, J. P. (2003). Effect of mixing on the rheology and particle characteristics of tungsten-based powder injection molding feedstock. *Mater Sci Eng A* 356:337–344. [https://doi.org/10.1016/S0921-5093\(03\)00146-1](https://doi.org/10.1016/S0921-5093(03)00146-1).
- [10] Kim, S. H., Kim, S. J., Park, S. J., et al. (2012). Rheological behavior of magnetic powder mixtures for magnetic PIM. *Korea Aust Rheol J* 24:121–127. <https://doi.org/10.1007/s13367-012-0014-1>.
- [11] Karatas, C., Kocer, A., Ünal, H. I., & Saritas, S. (2004). Rheological properties of feedstocks prepared with steatite powder and polyethylene-based thermoplastic binders. *J Mater Process Technol* 152:77–83. <https://doi.org/10.1016/j.jmatprotec.2004.03.009>.
- [12] Romero, A., & Herranz, G., (2017). Development of feedstocks based on steel matrix composites for metal injection moulding. *Powder Technol* 308:472–478. <https://doi.org/10.1016/j.powtec.2016.12.055>.
- [13] Krauss, V. A., Pires, E. N., Klein, A. N., & Fredel, M. C. (2005). Rheological properties of alumina injection feedstocks. *Mater Res* 8:187–189. <https://doi.org/10.1590/S1516-14392005000200018>.
- [14] Wei, W. J., Wu, R., Ho, S., (2000). Effects of pressure parameters on alumina made by powder injection moulding.pdf. 20:1301–1310.
- [15] Urtekin, L., Yılan, F., Uslan, İ. & Tuc, B. (2022). Seramik enjeksiyon kalıplama için iskelet bağlayıcı değişiminin reolojik özelliklerine etkisi. *Bilecik Şeyh Edebali Üniversitesi Fen Bilimleri Dergisi* , 9 (1), 314-323 . DOI: 10.35193/bseufbd.1020523.
- [16] Supati, R., Loh, N. H., Khor, K. A., & Tor, S. B. (2000). Mixing and characterization of feedstock for powder injection molding. *Mater Lett* 46:109–114. [https://doi.org/10.1016/S0167-577X\(00\)00151-8](https://doi.org/10.1016/S0167-577X(00)00151-8).
- [17] Thomas-Vielma, P., Cervera, A., Levenfeld, B., & Várez, A. (2008). Production of alumina parts by powder injection molding with a binder system based on high density polyethylene. *J Eur Ceram Soc* 28:763–771. <https://doi.org/10.1016/j.jeurceramsoc.2007.08.004>.
- [18] Subaşı, M., Safarian, A., & Karataş, Ç. (2019). An investigation on characteristics and rheological behaviour of titanium injection moulding feedstocks with thermoplastic-based binders. *Powder Metall* 62:229–239. <https://doi.org/10.1080/00325899.2019.1635305>.
- [19] Thavanayagam, G., & Swan, J. E. (2022). A new model for predicting the flow properties of Ti-6Al-4V-MIM feedstocks. *Powder Technol* 401:117306. <https://doi.org/10.1016/j.powtec.2022.117306>.
- [20] Ji, C. H., Loh, N. H., Khor, K. A., & Tor, S. B. (2001). Sintering study of 316L stainless steel metal injection molding parts using Taguchi method: Final density. *Mater Sci Eng A* 311:74–82. [https://doi.org/10.1016/S0921-5093\(01\)00942-X](https://doi.org/10.1016/S0921-5093(01)00942-X).
- [21] Wahi, A., Muhamad, N., & Zakaria, H. (2014). Optimization of 67% powder loading co-30cr-6Mo  $\mu$ MIM part by Taguchi method. *J Teknol (Sciences Eng)* 68:57–60. <https://doi.org/10.11113/jt.v68.2996>.
- [22] Chua, M. I. H., Sulong, A. B., Abdullah, M. F., & Muhamad, N. (2013). Optimization of injection molding and solvent debinding parameters of stainless steel powder (SS316L) based feedstock for metal injection molding. *Sains Malaysiana* 42:1743–1750.
- [23] Park, D. Y., Shin, D. S., Cho, H., & Park, S. J. (2017). Effects of material and processing conditions on powder-binder separation using the Taguchi method. *Powder Technol* 321:369–379. <https://doi.org/10.1016/j.powtec.2017.07.091>.
- [24] Wang, H. K., Wang, Z. H., & Wang, M. C. (2020). Using the Taguchi method for optimization of the powder metallurgy forming process for Industry 3.5. *Comput Ind Eng* 148:106635. <https://doi.org/10.1016/j.cie.2020.106635>.
- [25] Ahn, S., Park, S. J., Lee, S., et al. (2009). Effect of powders and binders on material properties and molding parameters in iron and stainless steel powder injection molding process. *Powder Technol* 193:162–169. <https://doi.org/10.1016/j.powtec.2009.03.010>.
- [26] Şap, E. (2021). Investigation of mechanical properties of Cu/Mo-SiCp composites produced with P/M, and their wear behaviour with the Taguchi method. *Ceram Int* 47:25910–25920. <https://doi.org/10.1016/j.ceramint.2021.05.322>.